Miller Range 13317

Polymict regolith breccia

32.25 g

Figure 1: *MIL 13317 as recovered in the field. Field photo image(s) courtesy of the* ***ANSMET*** *Program, Case Western Reserve Univ. and the Univ. of Utah.*

Introduction: The 2013-14 season ANSMET team recovered MIL 13317 which was classified as a lunar anorthositic breccia (**Figure 1**) and reported in the Antarctic Meteorite Newsletter (Satterwhite and Righter, 2015). MIL 13317 was found near the Marsh side glacier region at the southern edge of the southern icefield of the Miller Range (**Figure 2**). Cosmic ray exposure age data for MIL 13317 indicates it is not paired with any other MIL lunar meteorites (Nishiizumi and Caffee, 2013).

Petrography and Mineralogy: Although the initial description of MIL 13317 was "anorthositic" breccia (**Fig. 3, 4**), detailed studies of the multiple thin sections prepared in the early rounds of analysis demonstrated that this meteorite is really polymict and a mixture of both basaltic and anorthositic material. For example Zeigler et al. (2016), Shaulis et al. (2016) and Curran et al. (2016, 2019) all describe clasts of fine- and medium grained basalt, basaltic impact melt breccia, norite, more feldspathic impact melt breccias, and symplectites (**Figs. 5,6,7,8**). Clasts with symplectitic textures have been documented by Curran et al. (2019) and Robinson et al. (2019) – these are also common in lunar materials (**Fig. 8,9**). In addition, there are mineral fragments of pyroxene, olivine, and feldspar that are from all of the lithologies present as clasts. Glassy spherules were found in the matrix by all studies, indicating that this is a regolith breccia. Curran et al. (2019) document 20 different clasts in a single thin section, demonstrating the heterogeneity and diversity of lithologies present in this breccia (**Figure 7 and 8**).

Pyroxene and olivine Fe/Mn ratios fall as expected along a line defined by lunar samples, distinct from terrestrial or martian olivine and pyroxene (**Fig. 10**). Pyroxenes from basaltic clasts are FeO-rich as is typical for lunar basalt, while the pyroxenes in the impact melt clasts, norites, and granulites are more MgO-rich (**Fig. 11, 12, 13**). Plagioclase feldspar is overall more calcic in the feldspathic impact melt breccias and norites, while the basaltic materials are more sodic ranging down to An_{65} (**Fig. 11,13**). The combination of feldspar and pyroxene compositions demonstrate the affinity of the feldspathic clasts for ferroan anorthosite (FAN) materials defined in Apollo samples (**Fig. 14**). Trace element analyses of the minerals in a subset of clasts indicate feldspar affinity with lunar anorthosites, pyroxenes that are lower in REE than KREEP, and general overlap with a few lunar meteorites that are intermediate in composition between anorthosites and basalts (**Fig. 15**).

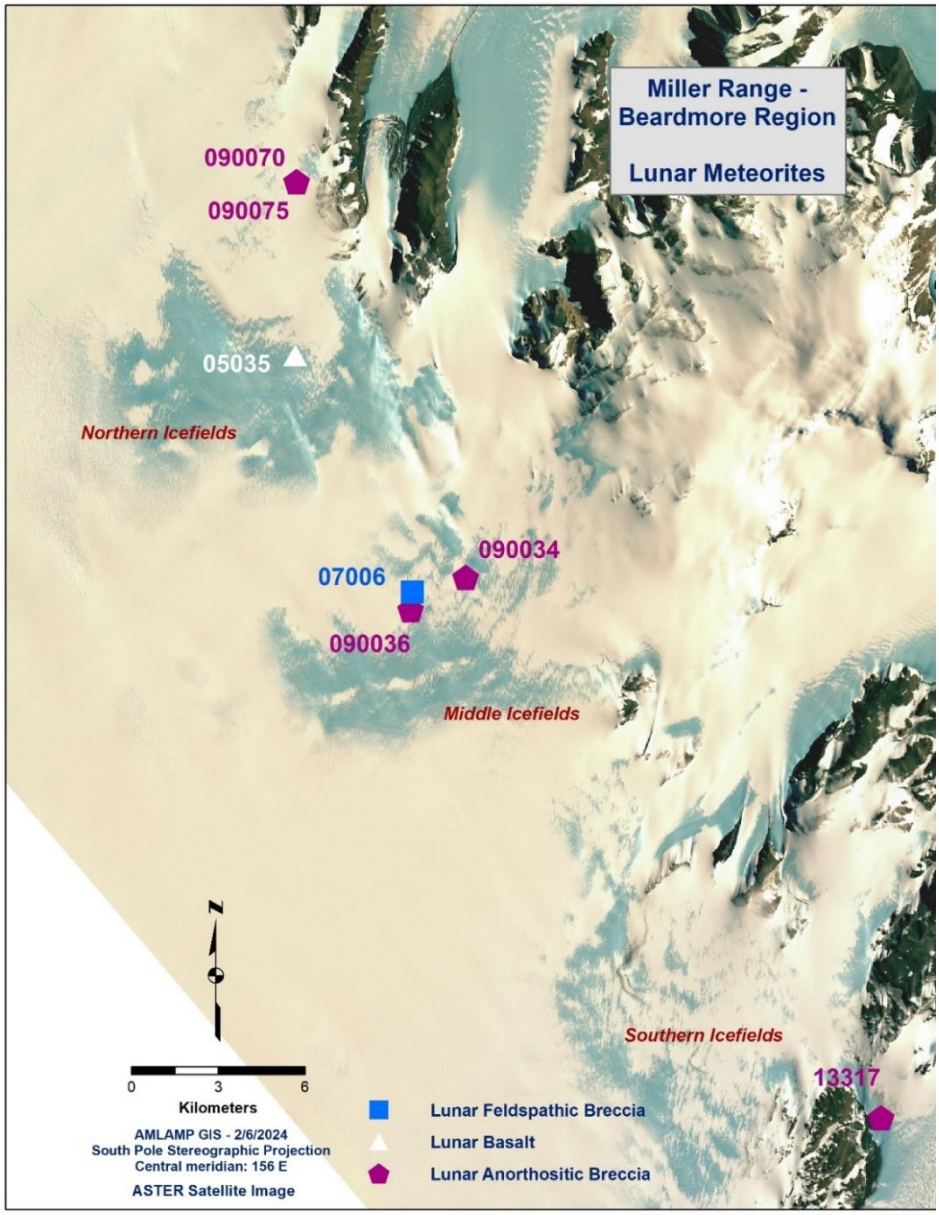

Figure 2: *Location of MIL 13317 lunar meteorite from the Miller Range 2013-14 ANSMET season, in the southern edge of the Southern Icefields (purple pentagon).*

Figure 3: *Macroscopic images of lunar meteorite MIL 13317, illustrating the brecciated interior that includes both basaltic (dark) and feldspathic (white) clasts and mineral fragments.*

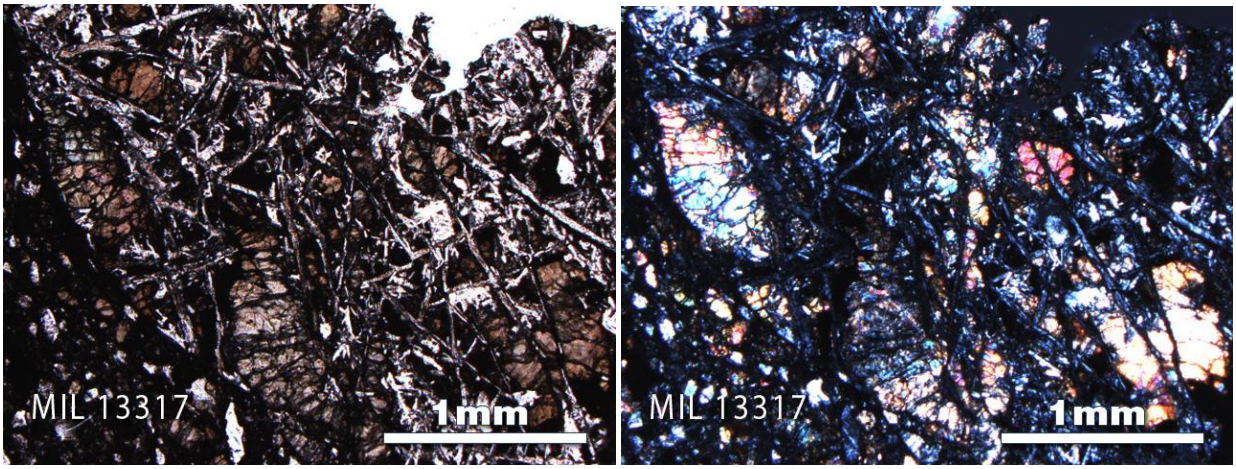

Figure 4: *Microscopic images of MIL 13317, illustrating the brecciated texture. Top left is plane polarized light and top right is cross polarized light images of one portion of the library section, whereas the bottom plane polarized light image shows the entire section including several different clast lithologies.*

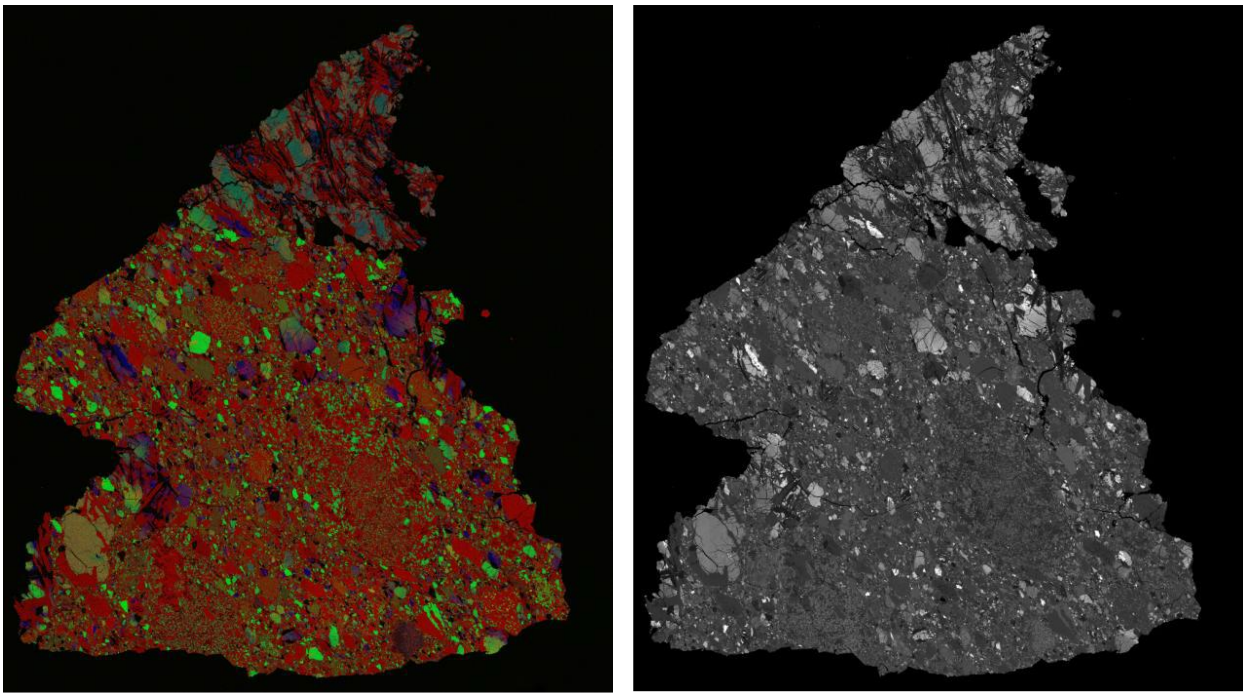

Figure 5: *RGB x-ray map (CaMgFe) of MIL 13317,13 (left) and BSE image of MIL 13317,13 (right). Field of view is 0.5 cm wide (figures from Zeigler et al., 2016).*

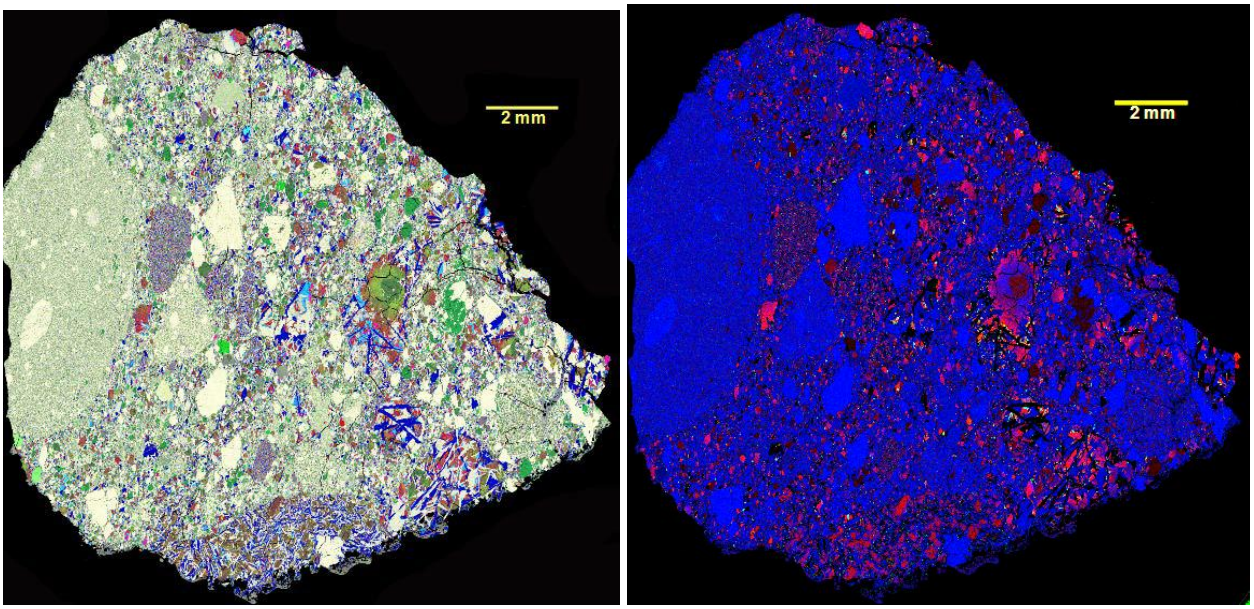

Figure 6: *False color element map of lunar anorthositic breccia MIL 13317,5 where Fe = red, Mg = green, Si = blue, Al = white, Ti = magenta, K = cyan, and Ca = yellow (left). False color map of MIL 13317,5 where Fe = red, P = green, and Ca = blue, used to identify zircon (green), apatite (cyan), and sulfide (yellow) minerals. Small apatite and zircon grains can be seen in several areas of the meteorite (figures from Shaulis et al., 2016).*

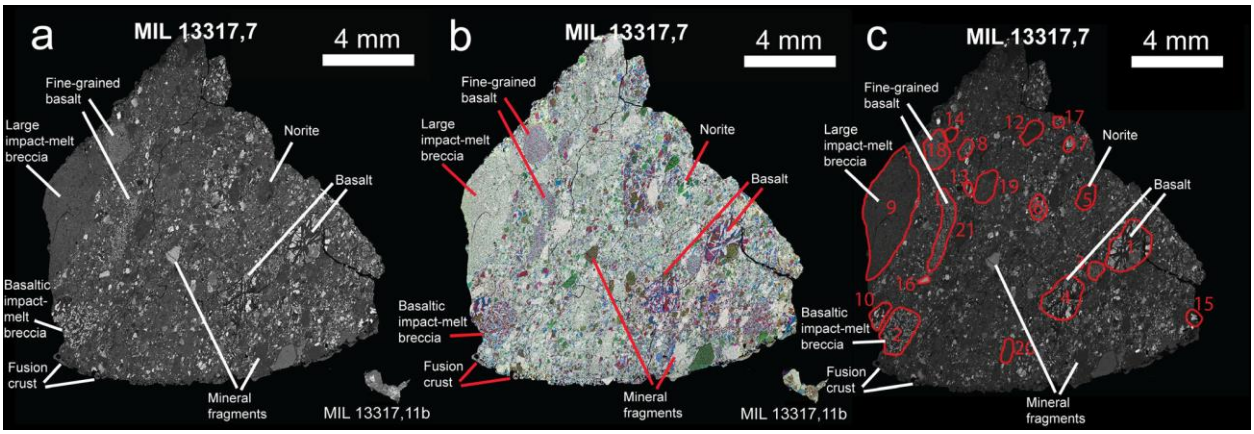

Figure 7: *a) Montaged backscattered electron images of thin section (MIL 13317,7) and polished block (MIL 13317,11a) of subsplits of MIL 13317. b) False-color element maps of two sections of MIL 13317 where colors correspond to: Ca = yellow (phosphates), Mg = green (pyroxene cores), Si = blue (silica), Fe = red (olivine, pyroxene rims), Al = white (plagioclase), Ti = pink (ilmenite and spinel), and K = cyan (k-feldspar). c) Backscattered electron image of MIL 13317,7 with clasts studied in this work outlined in red (figure from Curran et al. 2019).*

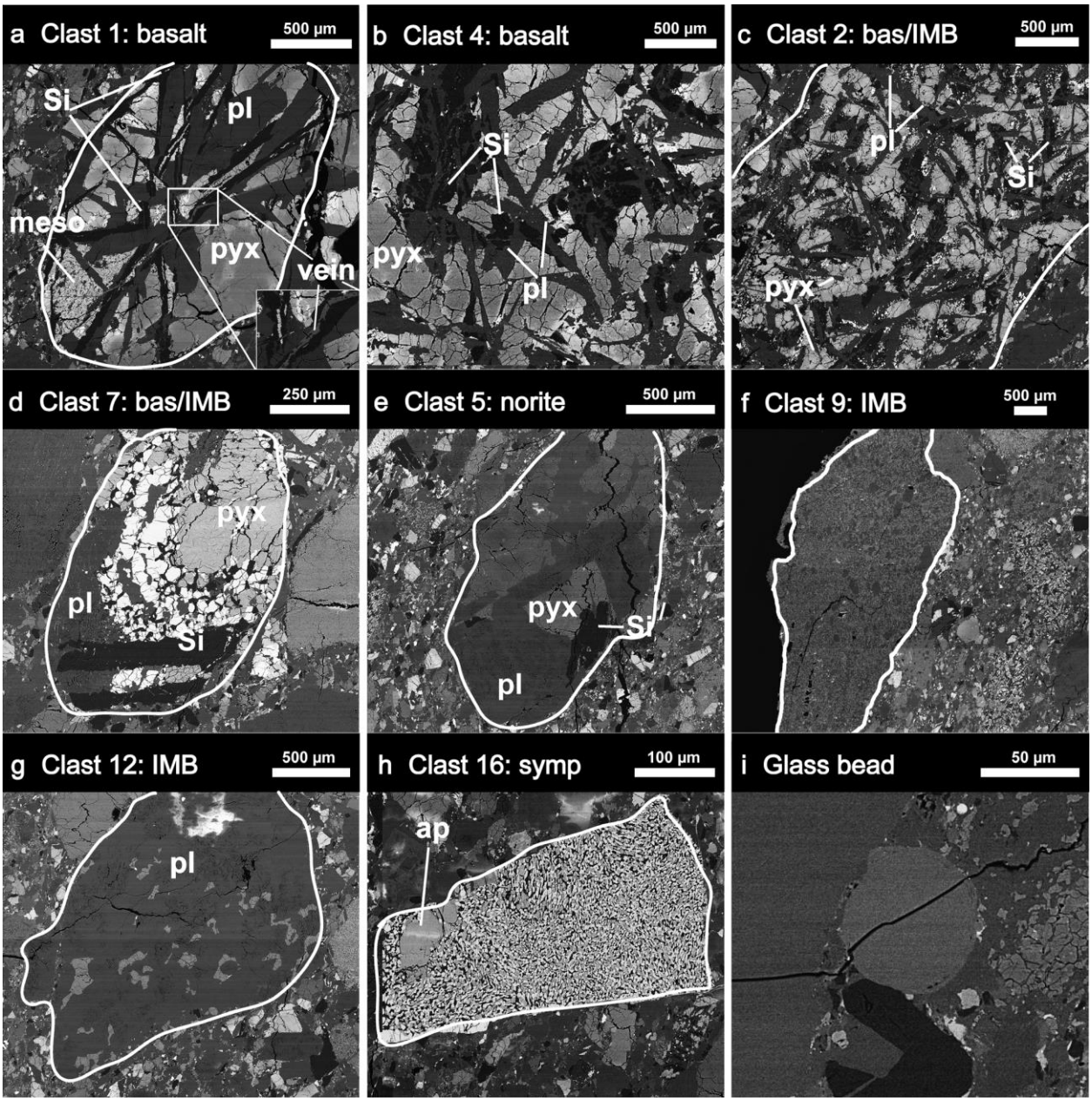

***Figure 8**: Backscattered electron images of clasts in MIL 13317,7. a) Clast 1 (basalt), (b) Clast 4 (basalt), (c) Clast 2 (basaltic impact melt breccia—bas/IMB), (d) Clast 7 (bas/IMB), (e) Clast 5 (norite), (f) Clast 9 (impact melt breccia, IMB), (g) Clast 12 (IMB), (h) Clast 16 (symplectite), and (i) a 50 µm glass bead. Mineral abbreviations: Si = silica; pl = plagioclase; pyx = pyroxene; ap = apatite; symp = symplectite; IMB = impact melt breccia; meso = mesostasis. Figure 1c shows the location of the different clasts in MIL 13317. Clasts compositions are featured in Figures 12 through 15 of this chapter (figures from Curran et al. 2019).*

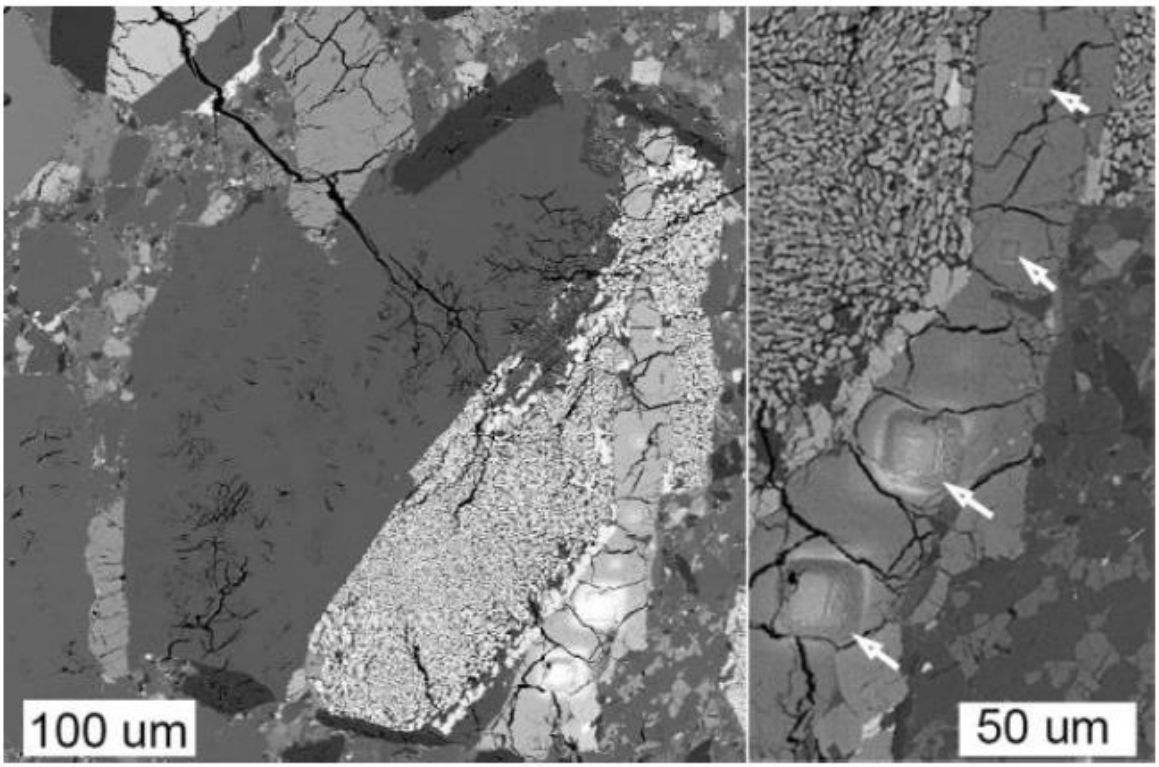

Figure 9: *BSE images of a clast in MIL 13317 ,23, with a large plagioclase bounded with symplectite, silica and Cl-apatite (left) and an apatite with SIMS analysis pits shown by arrows (right). The larger pits are from H isotope measurements, and the smaller pits from Cl isotope measurements (figure from Robinson et al. 2019).*

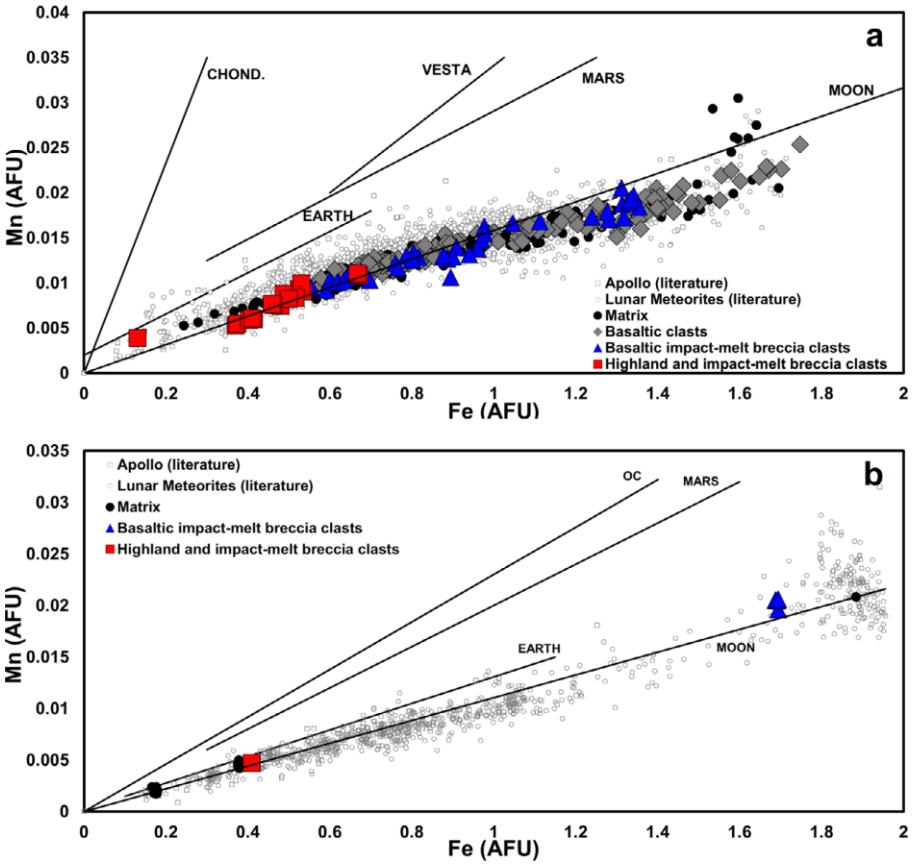

***Figure 10**: Fe/Mn versus Fe (atomic formula unit) for pyroxene (top) and olivine (bottom) from lithic materials and mineral clasts from MIL 13317 (from Curran et al. 2019).*

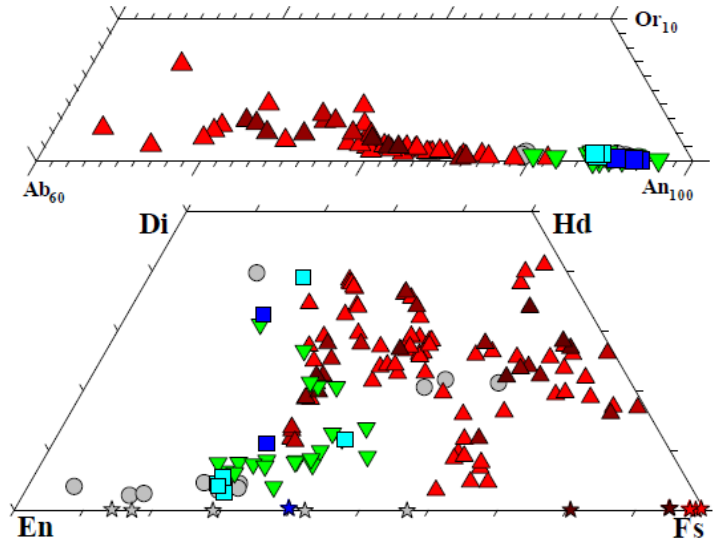

***Figure 11**: Top: A portion of the plagioclase ternary; Bottom: pyroxene quadrilateral with olivine compositions projected onto the En-Fs join (stars). Points in red are basaltic mineral clasts (different shades are different textures); blue are granulites, green are IMB, and grey are mineral clasts (figure from Zeigler et al., 2016).*

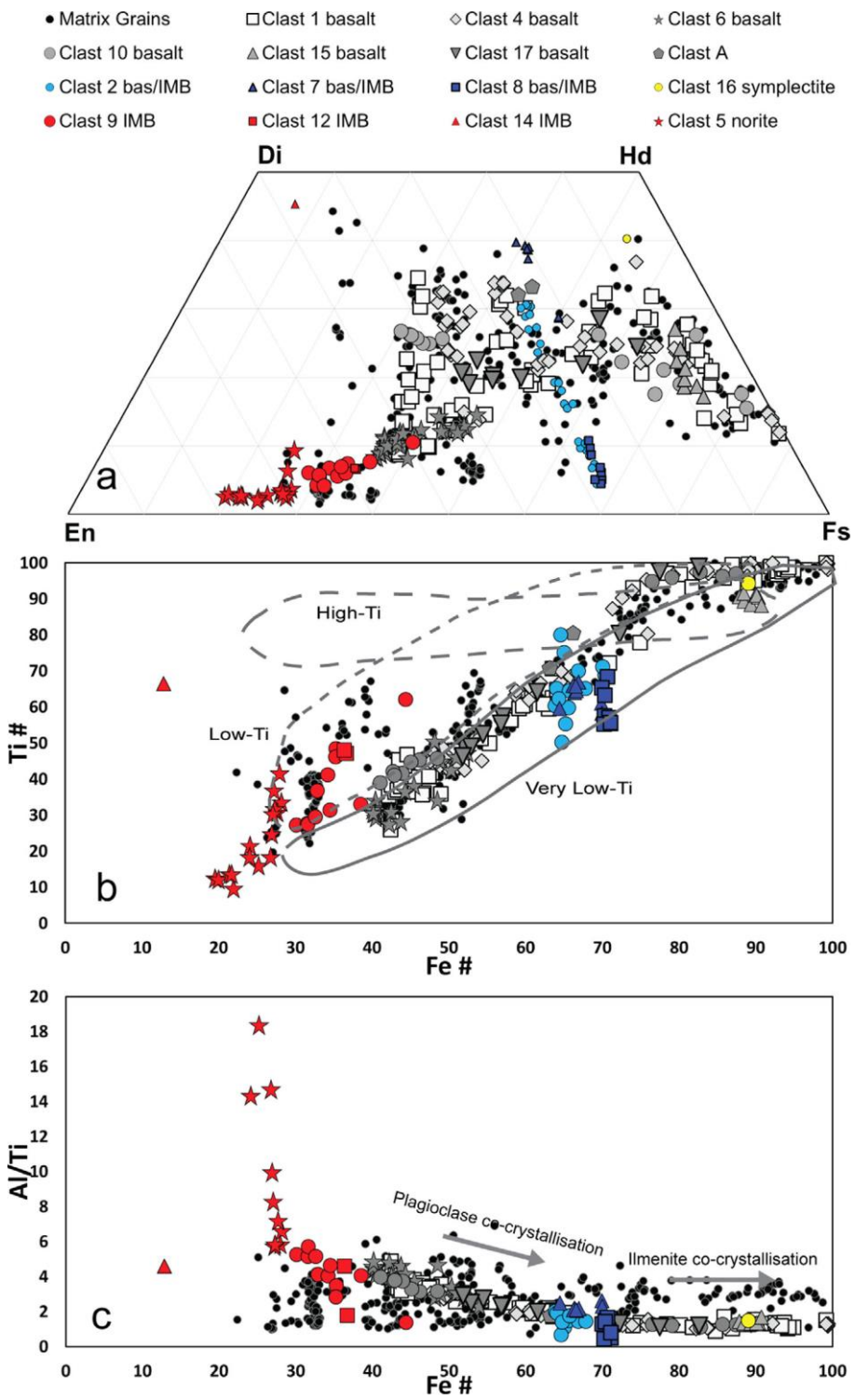

Figure 12: *Pyroxene mineral composition data for clasts and matrix in MIL 13317,7 and MIL 13317,11a. a) Pyroxene quadrilateral of these data. b) Fe# (atomic Fe/(Fe + Mg)*100) versus Ti# (atomic Ti/(Ti + Cr)*100). Fields show the extent of pyroxene composition in Apollo VLT, low-Ti and high-Ti mare basalts (from Bence and Papike 1972; Vaniman and Papike 1977; Dymek et al. 1975). c) Fe# (atomic Fe/(Fe + Mg)* 100) versus Al/Ti (atoms per formula unit) (figures from Curran et al., 2019).*

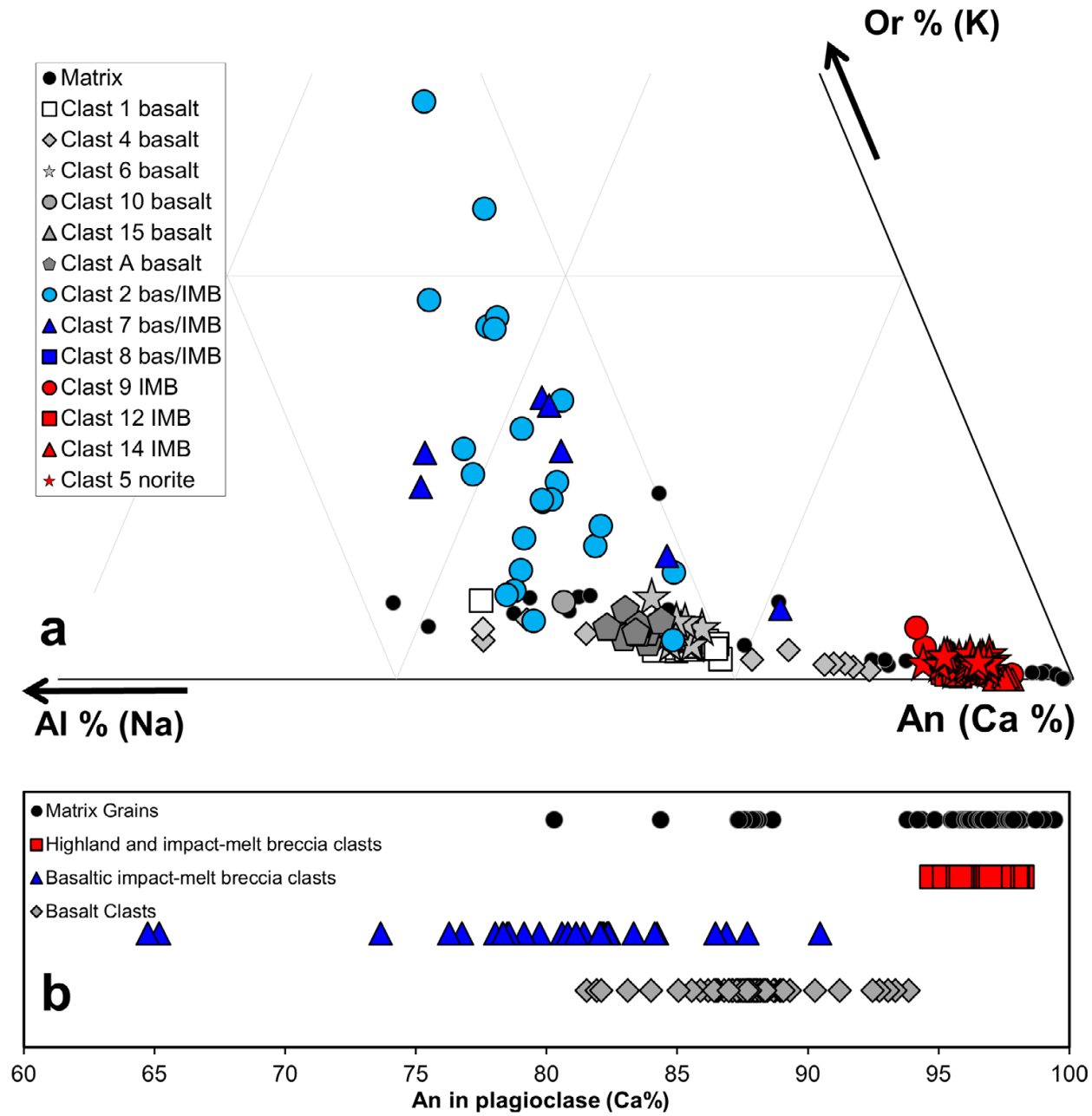

Figure 13: *Compositions of plagioclase grains in MIL 13317. a) Ternary diagram of anorthite (Ca), albite (Na), and orthoclase (K) for plagioclase in MIL 13317,7 and MIL 13317,11a. b) An content (atomic Ca/Ca + K + Na) for plagioclase in different clast types including basalt, impact melt breccia, highland clasts, and matrix mineral fragments (figures from Curran et al. 2019).*

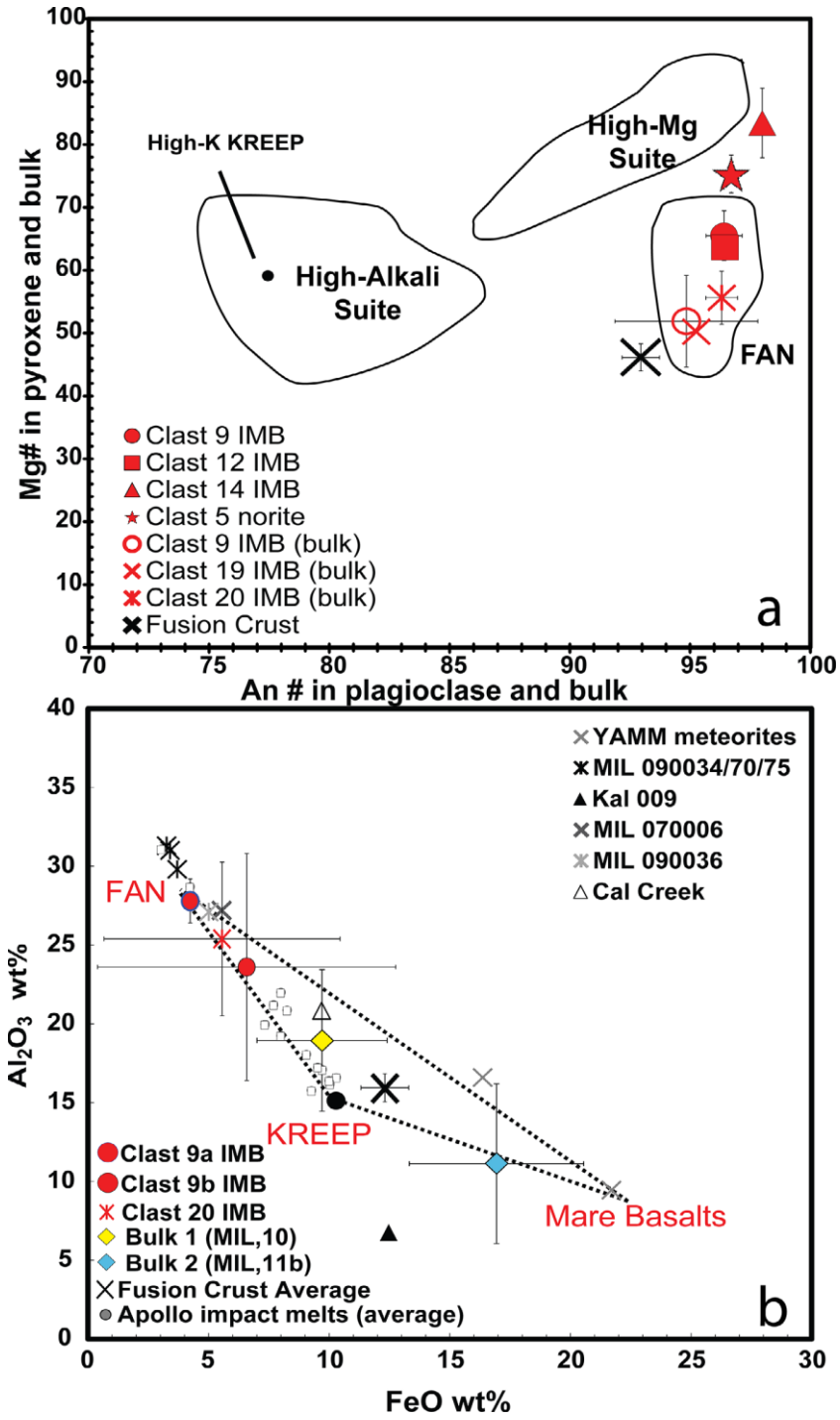

Figure 14: *a) Anorthite component (mol%) in plagioclase versus Mg# (=Mg/[Mg + Fe]*100) in mafic minerals in MIL 13317. Clast compositional relationships where the data points show the average An content in plagioclase (An#) and the Mg# content in pyroxene per clast. The error bars represent the total range of mineral chemistries determined per clast. Rock suite fields are from Shearer et al. (2006). b) Comparison of FeO (wt%) versus Al2O3 (wt%) showing the fusion crust composition for MIL 13317,7. MIL 13317 is compared to other Miller Range and the YAMM group of basaltic meteorites (data from Korotev and Zeigler 2014). MIL 13317 is also compared to another Th-rich meteorite Calcalong Creek (Hill and Boynton 2003) and Th-poor meteorite Kalahari 009 (figures from Curran et al. 2019).*

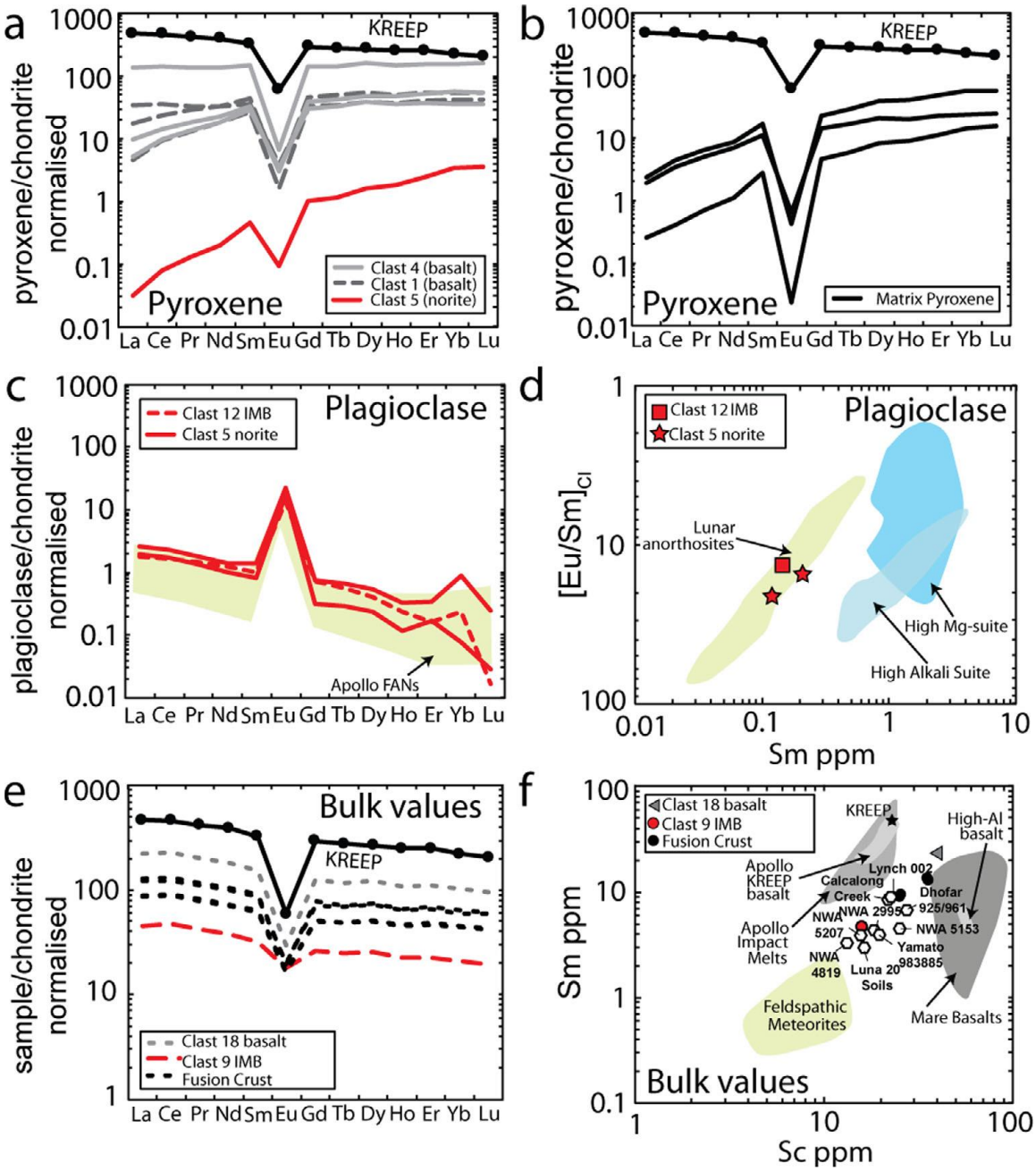

Figure 15*: a, b) Chondrite normalized (values from Anders and Grevesse 1989) pyroxene REE profiles for (a) pyroxene within basalt Clasts 1 and 4, and norite Clast 5. b) Pyroxene within the sample matrix. c) Chondrite normalized plagioclase REE profiles from impact melt breccia Clast 12 and norite Clast 5. d) Plagioclase [Eu/Sm]CI (CI chondrite normalized) versus Sm (ppm) from impact melt breccia Clast 12 and norite Clast 5 compared with data from different Apollo highland rock suites (data from Papike et al. 1996, 1997; Floss et al. 1998; Shervais and McGee 1998; Cahill et al. 2004). e) Chondrite-normalized REE profiles for basaltic Clast 18, impact melt breccia Clast 9, and the fusion crust. f) Sm (ppm) versus Sc (ppm) for basaltic clast 18, impact melt breccia Clast 9, and the fusion crust of MIL 13317,7. Lunar meteorites with intermediate compositions (from Korotev et al. 2009) have also been plotted for comparison. Fields of lunar rock types from Korotev et al. (2009). Bulk composition of high-K KREEP is shown for comparison in all plots (Warren 1989) (figures from Curran et al. 2019).*

Chemistry

MIL 13317 has glassy fusion crust that has been analyzed and may serve as an indication of bulk composition: 0.8 wt% TiO_2; 0.5 wt% Na_2O; 10.5 wt% FeO; Mg' = 52 (Zeigler et al., 2016). A dark-brown vesicular fusion crust is present on the MIL 13317,7 section, and displays LREE enrichment ([La/Sm]CI = 1.40), fractionated HREE profile ([Dy/Yb]CI = 1.15), Th-composition of 5.41 ppm, and a negative Eu-anomaly (Curran et al., 2019).

INAA analyses of MIL 13317 subsamples reveal a more mafic and incompatible trace element (ITE) - rich rock than other MIL lunar breccias. Compared to Calcalong Creek, NWA 4472/4485, and NWA 6687, subsamples of MIL 13317 increase in Sm and Na concentration with increasing Sc and Fe (**Figure 16**), suggesting MIL 13317 is not related to previously observed KREEPy lunar meteorites. Moreover, this trend suggests that MIL 13317 is a polymict breccia and a mix of (a) regolith which itself is a mixture of mare basalt and some KREEPy lithology, and (2) feldspathic material such as melt breccias and granulites. The mafic component cannot be just mare basalt because extrapolation of the FeO-Na_2O trend to 20% FeO, a typical value for mare basalt, leads to an absurdly high Na_2O concentration, 1.06%. Additionally, bulk compositions were determined from two chips MIL 13317,10 (Bulk 1) and MIL 13317,11b (Bulk 2). Bulk 1 is slightly more ferroan than the fusion crust and most similar to Apollo 17 regolith breccias (Mg# 29–47 and K_2O = 0.06–0.15 wt%). Bulk 2 has a higher K_2O content and is richer in Fe compared to the fusion crust and bulk 1. The fusion crust composition is intermediate between bulk 1 and 2 (from Curran et al. 2019).

Measurements of volatile elements in apatites from MIL 13317 have allowed a better understanding of their volatile content (H and Cl) (Robinson et al., 2019), and have indicated the possibility of heterogeneous volatile contents of the lunar interior (**Figure 17**).

Radiogenic age dating and mantle source constraints

One of the most interesting findings from MIL 13317 is the old age measured for some of the lithic clasts. Shaulis et al. (2016) report Pb-Pb ages of 4.270 and 4.276 Ga for baddeleyite and phosphates, respectively, and to 4.3518 Ga for phosphate and tranquillityite in MIL 13317 (**Fig. 18**). Curran et al. (2019) report a Pb-Pb ages of 4.315 to 4.365 Ga for zircon, baddeleyite, and apatite grains from matrix (and a few from a clast) in MIL 13317 (**Fig. 19**). U-Pb concordia ages for zircons and apatites range from 3.890 to 4.342 Ga in age, again demonstrating the older ages of materials in this breccia (**Fig. 20**). Finally, Pb-Pb isochrons for basaltic clasts yield an age of 4.332 Ga (**Fig. 21,22**). The high *mu* value derived from the Pb isotopic studies for basalt clast in MIL 13317 indicate values that overlap with other Apollo low Ti basalts indicating that the source region for these ancient basalts were not KREEP sources (**Fig. 23**), consistent with the KREEPy bulk signature coming from other components in the breccia, and indicating that the ancient basalts were unaffected by KREEP related processes.

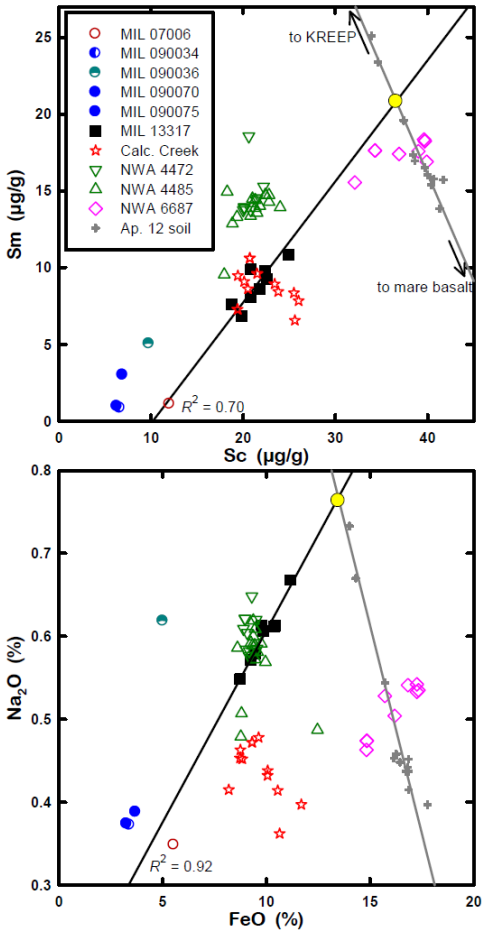

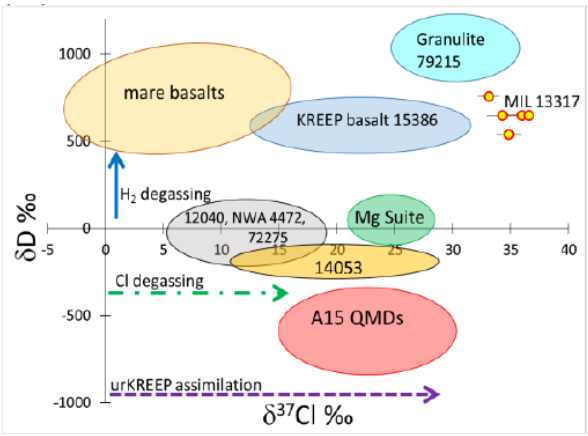

Figure 16 (left): *Comparison of MIL 13317 subsamples to subsamples of other meteorites of similar composition and to mean compositions of the other five MIL brecciated lunar meteorite stones, all of which are much more feldspathic. Unlike for Calcalong Creek, NWA 4472/4485, and NWA 6687, subsamples of MIL 13317 increase in Sm and Na concentration with increasing Sc and Fe (diagonal solid line). This trend suggests that the breccia is a mixture of (1) a regolith, represented hypothetically by the yellow circle, which itself is a mixture (as are the Apollo 12 soils) of mare basalt and some KREEPy lithology, and (2) feldspathic material (the melt breccias and granulites) with compositions like MIL 07006 and paired stones MIL 090034/70/75. The mafic component cannot be just mare basalt because extrapolation of the FeO-Na2O trend to 20% FeO, a typical value for mare basalt, leads to a absurdly high Na2O concentration, 1.06% (figures from Zeigler et al., 2016).*

Figure 17 (right): *δD (‰) vs. δ^{37}Cl (‰) for MIL 13317 ,23 apatites, compared to various other Apollo and lunar meteorite samples (figure from Robinson et al. (2019).*

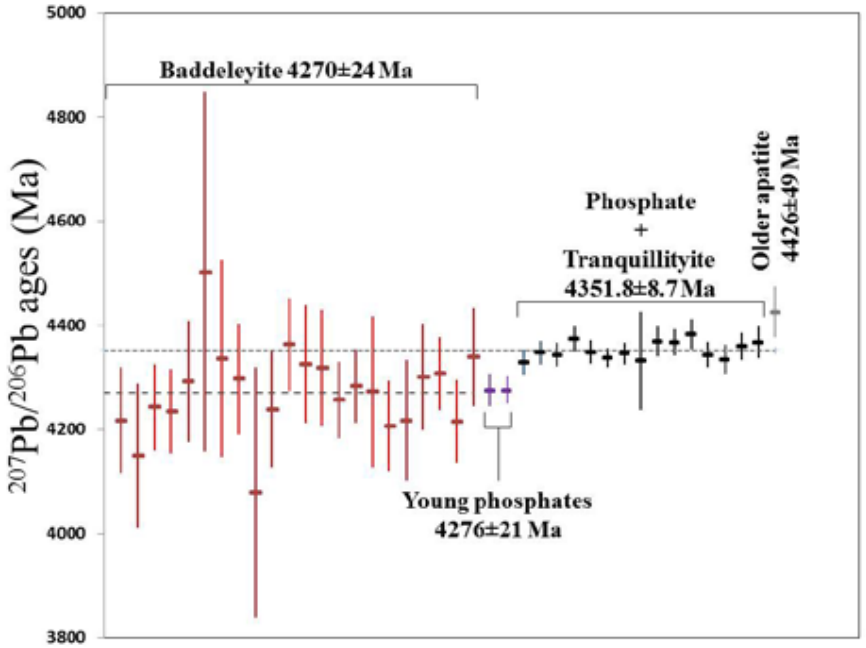

***Figure 18**: Pb-Pb ages of baddeleyite, Ca-phosphate phases of apatite and merrillite, and tranquillityite. The dashed line represents the weighted average age of baddeleyite (4270±24 Ma) and the dotted line represents the weighted average age of phosphate and tranquillityite (4351.8±8.7 Ma) (figure from Shaulis et al., 2016).*

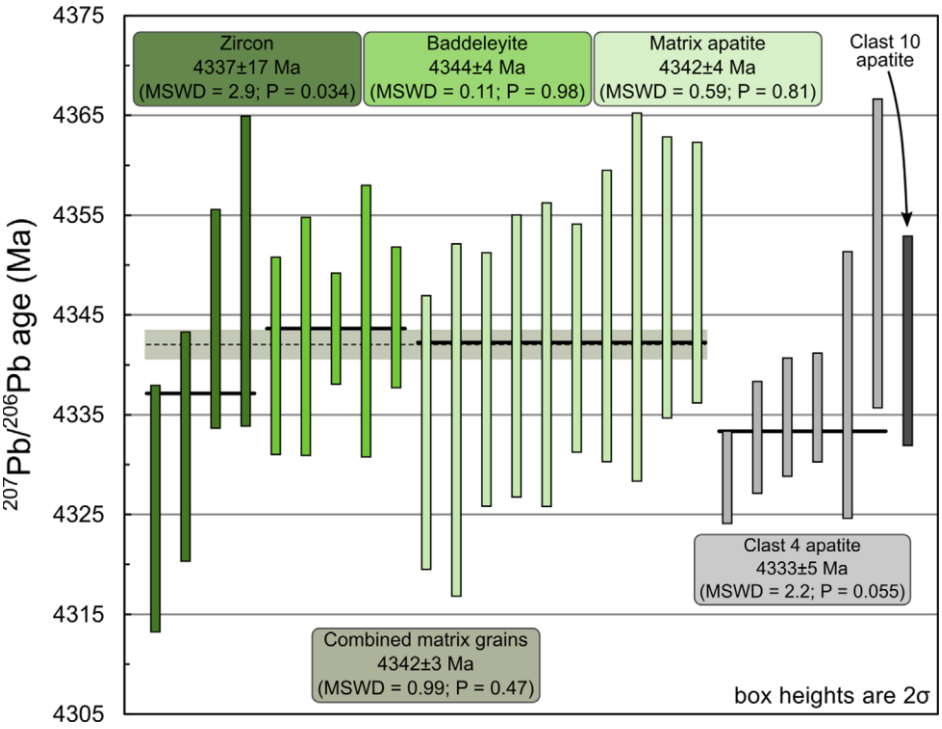

***Figure 19:** Terrestrial common Pb corrected $^{207}Pb/^{206}Pb$ ages for the zircon, baddeleyite, and apatite grains in MIL 13317. Weighted average $^{207}Pb/^{206}Pb$ ages have been indicated for each type of grain. The gray bar and dashed line represent the combined weighted average $^{207}Pb/^{206}Pb$ age for the matrix zircon, baddeleyite, and apatite grains. Uncertainties on the weighted average ages are stated at the 95% confidence level (figure from Curran et al. 2019).*

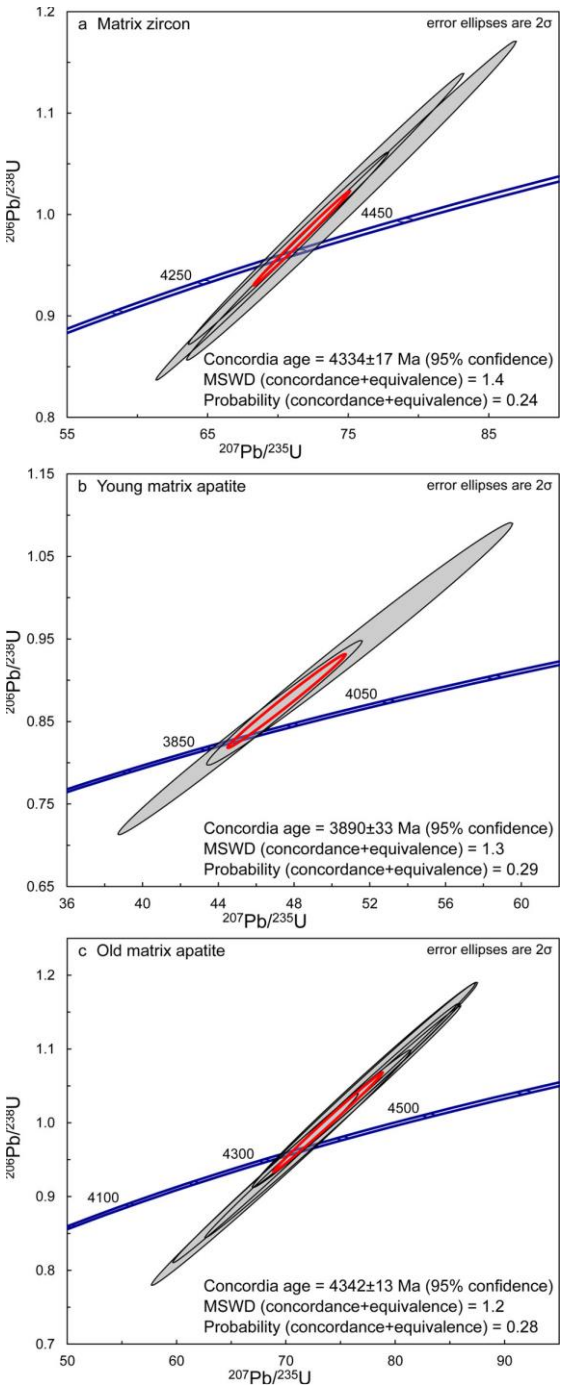

Figure 20: *Fig. 11. U-Pb concordia diagrams for data that are <10% discordant in the zircon (a), younger matrix apatite (b), and older matrix apatite (c) grains in MIL 13317. Uncertainties on the concordia ages are stated at the 95% confidence level and include the decay constant errors (figures from Curran et al. 2019).*

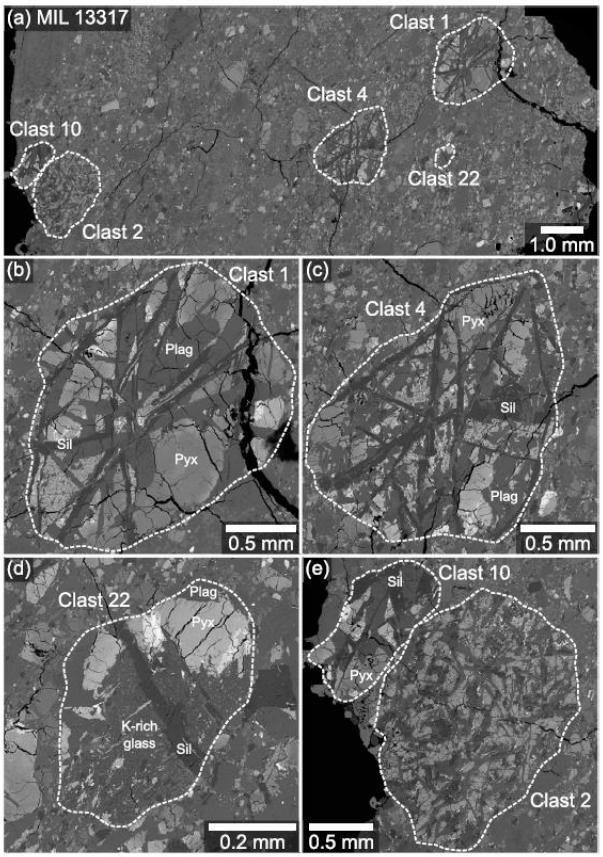

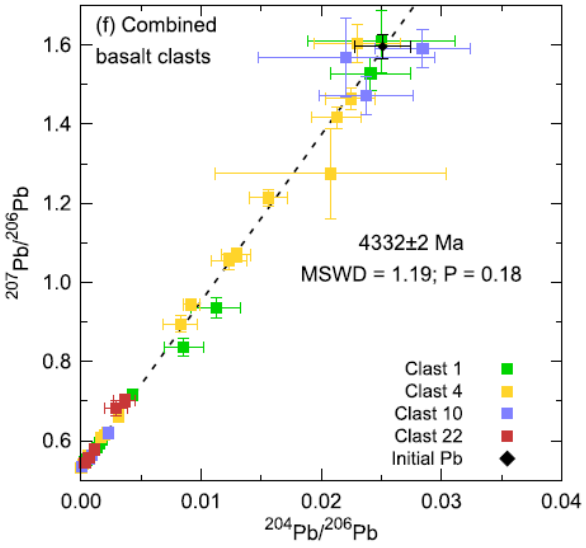

Figure 21 (left): *(a) Back Scattered Electron (BSE) image of the MIL 13317,7 thin section with the clasts analysed by Snape et al. (2018). More detailed images of the individual clasts are provided in panels (b–e). Plag – plagioclase; Pyx – pyroxene; Sil – silica (figure from Snape et al., 2018).*

Figure 22 (right): *A combined isochron and initial Pb isotopic composition was generated for the four basaltic clasts with ages of ~4330 Ma (f). Error bars represent 2σ uncertainties and uncertainties for the isochron dates are stated at the 95% confidence level (figure from Snape et al., 2018).*

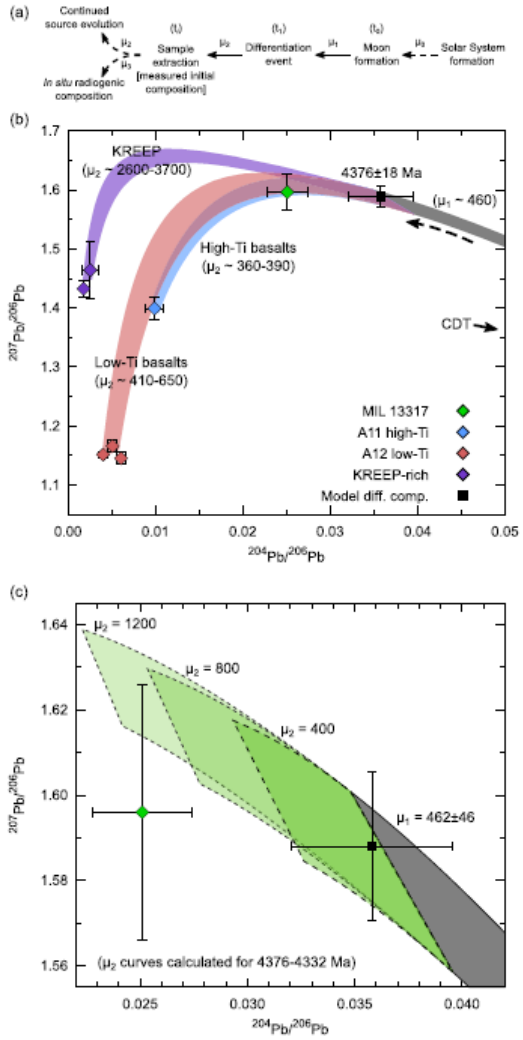

Figure 23: *(a) Schematic chart outlining the multi-stage Pb isotopic evolution model of Snape et al. (2016), the solid arrows indicate the stages represented in the model calculations. (b) Initial Pb isotopic composition of the MIL 13317 basalt clasts compared with the model of Snape et al. (2016). The model is calculated assuming lunar formation at 4500 Ma and a primitive starting composition of Canyon Diablo Troilite (CDT; Göpel et al., 1985). In the model, an undifferentiated bulk Moon with a μ1-value of ~460 evolves until 4376 ±18Ma. The mantle sources of the main Apollo basaltic suites can all be modelled as originated from the model differentiation composition with distinct μ2-values. The initial Pb isotopic compositions of the Apollo 11 high-Ti basalt 10044, Apollo 12 low-Ti basalts 12038, 12039 and 12063, the KREEP-rich Apollo 14 high-Al basalts 14072 and the KREEP basalt 15386 have also been plotted for comparison (data originally presented in Snape et al., 2016). (c) Focusing just on the region between the model differentiation point at 4376 ±18Ma and the MIL 13317 basalts, the μ2-value (850 ±130; 2σ) necessary to form this composition within the model framework, would have been more similar to that attributed to the Apollo mare basalt sources than that of the high-μKREEP basalt sources. Error bars and the Pb growth curve fields represent 2σ uncertainties. (figures from Snape et al. 2018).*

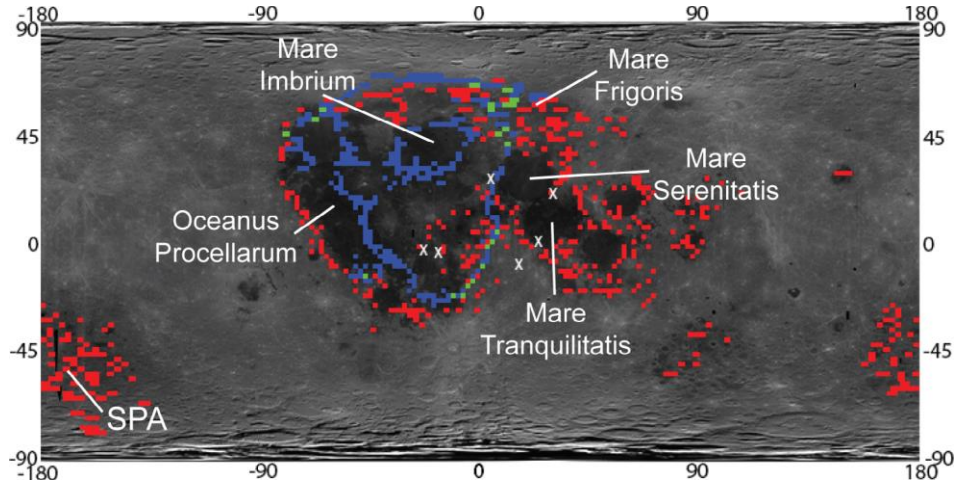

Figure 24*: Identification of lunar regolith with compositional similarities to MIL 13317. Compositional matches are FeO = red, Th = blue, and for both FeO and Th = green. The data here show the MIL 13317 is most compositionally similar in terms of surficial FeO and Th to the PKT terrane, with Mare Frigoris, southeast region of the PKT, or the northwest region of Oceanus Procellarum the most compositionally similar regions. Data are overlaid on Clementine albedo images of the Moon in a cylindrical projection (from Curran et al. 2019).*

Splits of MIL 13317 as of January 2024 (not including attrition)

split	mass	parent	form	PI-1	PI-2	current
0	15.65	-	DOC PC	-	-	JSC
1	2.575	0	PB	-	-	JSC
2	0.01	1	TS	SI	-	SI
4	0.01	1	TS	-	-	JSC
5	0.01	1	TS	Kring	-	Kring
6	0.01	1	TS	Zeigler	-	Zeigler
7	0.01	1	TS	Joy	Curran	Curran
8	0.599	0	PB	-	-	JSC
9	0.416	0	CPS	Korotev	-	JSC
10	0.058	0	CPS	Joy	-	SI
11	0.159	0	CPS	Joy	-	SI
13	0.01	8	TS	Zeigler	-	Zeigler
14	5.92	0	DOC CP	-	-	JSC
15	1.8	0	DOC CP	-	-	JSC
16	3.56	0	CPS+FI	-	-	JSC
18	0.39	15	EXT CP	Nishiizumi	-	Nishiizumi
19	0.25	15	INT CP	Nishiizumi	-	Nishiizumi
20	0.74	15	CPS+FI	-	-	JSC
23	0.01	1	TS	Kring	-	Kring

Summary

Studies of the petrology and geochemistry of MIL 13317 have shown that it is a mixture of basaltic and feldspathic materials and is a polymict regolith breccias (Shaulis et al., 2016; Ziegler et al., 2016; Curran et al., 2019; Robinson et al., 2019). Feldspathic impact melt breccias and norites have an affinity to FANs. The basaltic materials were derived from an ancient KREEP-free mantle and have ages as old as 4.4 Ga. Comparison of bulk FeO and Th in MIL 13317 to global lunar geochemical data shows a likely source near the Procellarum KREEP Terrane, with the best matches to both FeO and Th between Mare Imbrium and Mare Frigoris or SE of Mare Tranquilitatis (**Fig. 24**).

References:

Nishiizumi, K., & Caffee, M. W. (2013) Relationships among six lunar meteorites from Miller Range, Antarctica based on cosmogenic radionuclides. In *44th Annual Lunar and Planetary Science Conference* (No. 1719, p. 2715).

Curran, N.M., Joy, K.H., Snape, J.F., Pernet-Fisher, J.F., Gilmour, J.D., Nemchin, A.A., Whitehouse, M.J., and Burgess, R. (2019) The early geological history of the Moon inferred from ancient lunar meteorite Miller Range 13317. *Meteoritics & Planetary Science*, 54, 1401-1430, doi: 10.1111/maps.13295.

Robinson, K. L., Nagashima, K., Huss, G. R., Taylor, G. J., & Kring, D. A. (2019) An Ancient KREEP-Poor, Chlorine-37-Rich Source Within the Moon. In *50th Annual Lunar and Planetary Science Conference* (No. 2132, p. 2063).

Satterwhite, C. E. and Righter, K. (2015) Ant. Met. Newsl. 38 no. 2.

Shaulis, B. J., Kring, D. A., Lapen, T. J., & Righter, M. (2016) Petrology and distribution of U-Pb ages in lunar meteorite breccia Miller Range (MIL) 13317. In *47th Annual Lunar and Planetary Science Conference* (No. 1903, p. 2027).

Snape, J. F., Curran, N. M., Whitehouse, M. J., Nemchin, A. A., Joy, K. H., Hopkinson, T., ... & Kenny, G. G. (2018) Ancient volcanism on the Moon: Insights from Pb isotopes in the MIL 13317 and Kalahari 009 lunar meteorites. Earth and Planetary Science Letters, 502, 84-95.

Zeigler, R. A., & Korotev, R. L. (2016) Petrography and Geochemistry of Lunar Meteorite Miller Range 13317. In *47th Annual Lunar and Planetary Science Conference* (No. 1903, p. 2554).

Kevin Righter, April 2024